ACS Partner Journal

Journal of the American Society for Mass Spectrometry

pubs.acs.org/jasms

Research Article

Rapid Screening and Quantification of PFAS Enabled by SPME-DART-MS

Ronald V. Emmons, William Fatigante, Aghogho A. Olomukoro, Brian Musselman, and Emanuela Gionfriddo*

Cite This: *J. Am. Soc. Mass Spectrom.* 2023, 34, 1890−1897

Read Online

ACCESS | Metrics & More | Article Recommendations | Supporting Information

ABSTRACT: Per- and polyfluoroalkyl substances (PFAS), an emerging class of toxic anthropogenic chemicals persistent in the environment, are currently regulated at the low part-per-trillion level worldwide in drinking water. Quantification and screening of these compounds currently rely primarily on liquid chromatography hyphenated to mass spectrometry (LC-MS). The growing need for quicker and more robust analysis in routine monitoring has been, in many ways, spearheaded by the advent of direct ambient mass spectrometry (AMS) technologies. Direct analysis in real time (DART), a plasma-based ambient ionization technique that permits rapid automated analysis, effectively ionizes a broad range of compounds, including PFAS. This work evaluates the performance of DART-MS for the screening and quantification of PFAS of different chemical classes, employing a central composite design (CCD) to better understand the interactions of DART parameters on their ionization. Furthermore, in-source fragmentation of the model PFAS was investigated based on the DART parameters evaluated. Preconcentration of PFAS from water samples was achieved by solid phase microextraction (SPME), and extracts were analyzed using the optimized DART-MS conditions, which allowed obtaining linear dynamic ranges (LDRs) within 10 and 5000 ng/L and LOQs of 10, 25, and 50 ng/L for all analytes. Instrumental analysis was achieved in less than 20 s per sample.

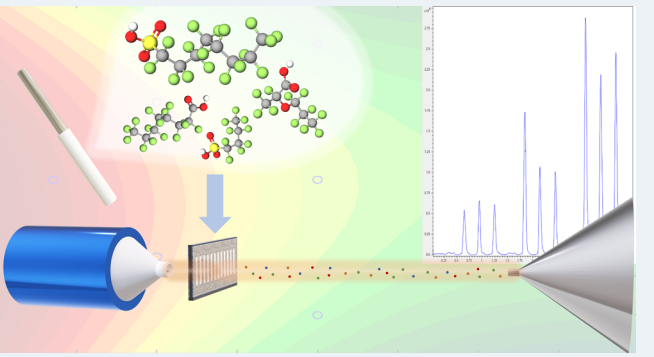

INTRODUCTION

The analysis of per- and polyfluoroalkyl substances (PFAS) has become critical for routine environmental monitoring, as their presence in drinking water, seafood, environmental, biological, and food samples has been repeatedly documented throughout the world.[1] Used in various industrial and consumer products such as firefighting foam, nonadhesive cookware, and stain-resistant materials,[2−4] PFAS are highly persistent in the environment due to their remarkable chemical stability. Studies have shown these chemicals to contribute toward various human health risks such as diabetes and high blood pressure;[5−8] in fact, several regulatory agencies are proposing to continuously lower established legally enforceable levels, called Maximum Contaminant Levels (MCLs), in drinking water. The World Health Organization (WHO) has recommended limits of 100 parts-per-trillion (ng/L) for perfluorooctanoic acid (PFOA) and perfluorooctanesulfonic acid (PFOS), two commonly detected legacy PFAS.[9] The US Environmental Protection Agency (EPA) set limits of 70 ng/L for these compounds in 2016, and in 2023, the limits were set at even lower concentrations: 4 ng/L for PFOA and 4 ng/L for PFOS.[10] In addition, this health advisory also set limits of 10 ng/L for hexafluoropropylene oxide dimer acid (GenX) and 2000 ng/L for (perfluoro-1-butanesulfonate) PFBS. In response to the ever-increasing need for the ultratrace analysis of PFAS, highly sensitive techniques must be developed with an increasing focus on higher sample throughput for both screening and quantification of these contaminants.

The chemical structure of PFAS varies across different classes, as their hydrophobic fluorinated alkyl chain is bound to different hydrophilic groups. Common polar groups consist of carboxylic acid or sulfonic acid moieties, while recently developed PFAS also contain ether linkages to promote environmental degradation.[11,12] As such, analytical approaches must take these major chemical classes into account. Conventionally, analysis of PFAS is performed utilizing LC-MS/MS techniques.[8,13−15] While these methods are highly sensitive and allow effective separation of isomeric species and quantification, alternative techniques such as direct ambient mass spectrometry (AMS) can enable higher sample throughput, which is ideal for screening purposes.[16] The

Special Issue: Focus: 2023 Emerging Investigators

Received: March 7, 2023
Revised: May 3, 2023
Accepted: May 10, 2023
Published: June 1, 2023

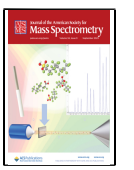

https://doi.org/10.1021/jasms.3c00088
J. Am. Soc. Mass Spectrom. 2023, 34, 1890−1897

plasma-based AMS technique direct analysis in real time (DART) enables high throughput screening and quantification of various classes of molecules for both positively and negatively ionized species.[17−22] Furthermore, there has been recent interest in the DART analysis of PFAS, with results from Cody and Maleknia demonstrating robust ng/L level quantification of PFOA and the screening of various other PFAS such as PFOS, using coated glass capillaries (CGCs) with octadecylamine as an extraction phase for PFAS.[23] In fact, many developed AMS methods benefit from analyte preconcentration prior to instrumental analysis.[24,25] Previous work from our research group has demonstrated the use of solid phase microextraction (SPME) devices composed of hydrophilic−lipophilic balance−weak anion exchange particles embedded in polyacrylonitrile (HLB-WAX/PAN) as an ideal strategy for the preconcentration of multiple classes of PFAS, allowing sub-ng/L detection when coupled with LC-MS/MS.[15,26]

To the authors' knowledge, there have been few studies coupling SPME and DART for the quantitative analysis of PFAS.[23] Furthermore, the effects of various parameters affecting the DART ionization and detection of multiclass PFAS have not yet fully evaluated. This work employs a multivariate experimental design, central composite design (CCD), to better understand the interactions and roles of each parameter involved in PFAS ionization mechanisms. Four model analytes, PFOA, PFOS, GenX, and PFBS, were studied due to their varying physicochemical properties and relevance in current regulatory efforts.

MATERIALS AND METHODS

Chemicals. PFAS standards (PFOA, PFOS, PFBS, and GenX) were purchased from AccuStandard (New Haven, CT, USA). Their physicochemical data and structures can be found in Table S1 and Figure S1, respectively. Isotopically labeled internal standards ($^{13}C_8$−PFOA, $^{13}C_8$−PFOS, $^{13}C_3$−GenX) were purchased from Wellington (Ontario, Canada). Ammonium formate was obtained from Fisher Scientific (Waltham, MA, USA). HLB-WAX particles were purchased from Waters Corporation (Milford, MA) and PAN from Millipore Sigma (Bellefonte, PA, USA). *N*,*N*-Dimethylformamide was obtained from Acros Organics (Pittsburgh, PA, USA). Nitinol wire was purchased from Component Supply Company (Sparta, TN) and stainless-steel blades from Yarder Manufacturing Company (Toledo, OH). HLB-WAX/PAN SPME devices were manufactured according the methods outlined in previous works.[15,26] Ultrapure water was collected from a Nanopure Infinity System (Barnstead, Thermo Fisher Scientific).

Instrumentation. Method optimization, fragmentation studies, and CCD experiments were performed on a DART-SVP (Bruker Scientific LLC, Billerica, MA, USA) hyphenated to an LTQ XL ion trap mass spectrometer (MS) (Thermo Fisher Scientific, San Jose, CA, USA). MS parameters include a scan of 80 to 520 m/z with a 10 ms maximum injection time and 1 μscan and the MS set to a "normal" speed setting. Quantification was performed on a DART-JS hyphenated to a Bruker EVOQ Elite (Bruker Scientific LLC, Billerica, MA, USA). MS/MS conditions are described in Table S2.

Sample Preparation. The sample preparation procedure and development of SPME devices were adapted from Olomukoro et al.[15,26] SPME devices (fibers and blades) consisting of hydrophilic−lipophilic balance particles embedded in polyacrylonitrile (HLB-WAX/PAN) were used (Figure S2). The extraction procedure was carried out in 2 mL glass vials with a PTFE cap, with a sample volume of 1 mL ultrapure water and agitation of 1000 rpm (vortex agitation) for 30 min. Subsequently, the device was desorbed for 20 min in a 500 μL plastic vial containing 150 μL of 80:20 methanol:water desorption solution with 0.5% (w:w) ammonium formate for the SPME fiber extraction. For SPME blades, desorption was performed in 250 μL of methanol:water desorption solution with 2% (w:w) ammonium formate. All calibration levels were prepared in triplicate.

Direct Analysis in Real Time. Unless otherwise noted, DART optimization was carried out by spiking 5 μL of a 1 ppm solution of PFAS in methanol onto a QuickStrip (Figure S3) in triplicate. A circumscribed central composite design (CCD) was performed with three major variables (e.g., electric grid voltage, plasma heater temperature, interface pressure).[27−29] Optimal DART parameters were found to be −50 V for the electric grid and 897 mbar for the interface pressure. Plasma heater values were optimized separately for carboxylic- and sulfonic-acid-containing PFAS, with optimal temperatures being 250 and 400 °C for carboxylic and sulfonic acids, respectively (Table S3). For each parameter investigated, lower and upper levels of the design were chosen based on the operable conditions of the DART system, the design of the CCD being described in Table S4. Each level of the experiment was performed randomized in triplicate.

Data Analysis. Data obtained for optimization and evaluation of DART and sample composition parameters were obtained and integrated using Xcalibur software (Thermo Fisher Scientific, San Jose, CA, USA) and processed using Excel 2016 (Microsoft Corporation, Albuquerque, NM, USA). The circumscribed CCD model was developed, visualized, and evaluated using STATISTICA 12.0 (StatSoft, Tulsa, USA). Quantitative data for the method calibration was obtained and integrated using tqControl software (Bruker Scientific LLC, Billerica). Prism 5 (Graphpad Software, La Jolla, CA, USA) was used to plot calibration curves.

RESULTS AND DISCUSSION

In-Source Fragmentation. There are multiple parameters that influence DART ionization of analytes, primarily plasma temperature, plasma makeup (typically helium or nitrogen gas), electric grid voltage, and the interface pressure of the DART-MS interface. To study these effects, the four model PFAS were chosen due to their physicochemical diversity. PFOS and PFBS both have terminal sulfonic acid moieties but contain carbon chains with different lengths (PFOS: $C_8HF_{17}O_3S$, PFBS: $C_4HF_9O_3S$), while PFOA has a terminal carboxylic acid group ($C_8HF_{15}O_2$) and GenX has both a terminal carboxylic acid moiety and an internal ether linkage ($C_6HF_{11}O_3$). Initial findings demonstrated a strong degree of in-source fragmentation for these analytes (Figure S4). The degree of in-source fragmentation is minor for the sulfonic acids, while the fragmentation of the carboxylic acids was pronounced enough to remove up to four CF_2 subunits of PFOA. This phenomenon is not entirely unexpected, as PFAS fragmentation is thought to proceed through an "unzipping mechanism"[30] or a continuous fragmentation due to rapid fluorine shifts[31] following initial decarboxylation or loss of SO_3. This results in a series of fragments with the removal of CF_2, C_2F_4, C_3F_6, etc. along a linear chain, with branched chains also being fragmented (in the case of GenX, a loss of CF_3−CF_1 is observed). While there have been attempts to minimize this

https://doi.org/10.1021/jasms.3c00088
J. Am. Soc. Mass Spectrom. 2023, 34, 1890−1897

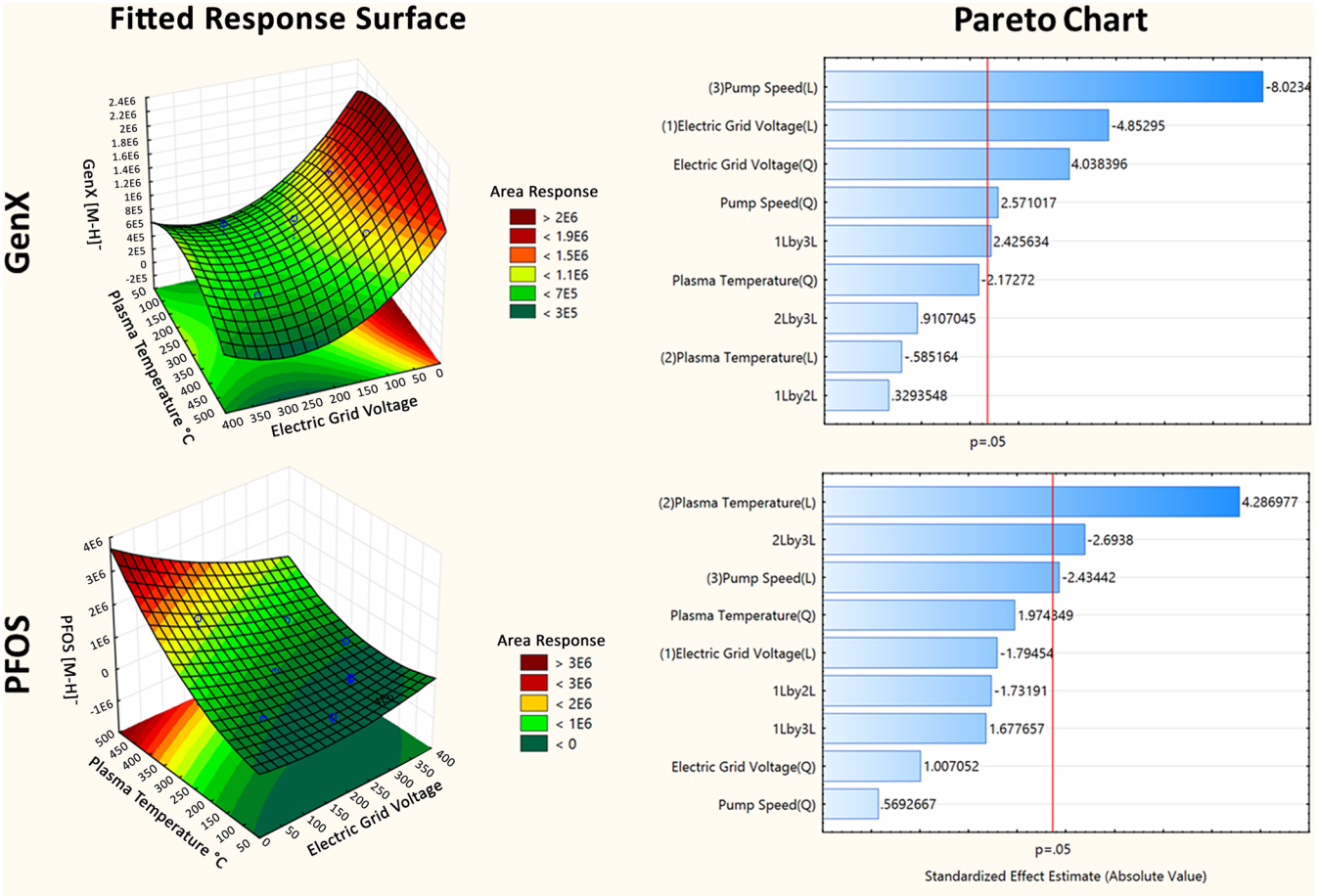

Figure 1. Central composite design of GenX and PFOS using helium plasma, with interface pressure kept constant (897 mbar). Electric grid voltage is plotted by absolute values.

characteristic fragmentation pattern,[32] loss in sensitivity of the $[M - H]^-$ ion is primarily associated with the perfluoroethercarboxylic acids. This is exacerbated by heat in the ion source; in fact, decarboxylation can occur at standard operating temperatures of both electrospray ionization (ESI) and DART. Because of this, most developed methods using ESI opt to forego monitoring the $[M - H]^-$ ion of perfluoroethercarboxylic acids such as GenX and instead select its more prominent $[M - H - CO_2]^-$ ion.[15] This phenomenon has been demonstrated to be beneficial in DART-TOF-MS analysis, with the fragmentation of PFOA accurately identified by its unique Kendrick mass defect.[23] In this work, all model analytes exhibited in-source fragmentation as a result of removal of CO_2 or SO_3 by the heated plasma stream with the exception of PFOS. While sulfonic-acid-containing PFAS demonstrated better relative $[M - H]^-$ stability, carboxylic-acid-containing PFAS demonstrated a larger degree of this fragmentation at higher plasma temperatures. Thus, optimization experiments were carried out monitoring $[M - H]^-$ as the quantitative ion for PFOS, PFBS, and PFOA and $[M - H - CO_2]^-$ for GenX.

Central Composite Design. Due to the initial observation of in-source fragmentation for all studied model PFAS, a multiparameter approach that accounts for the selected quantitative ions across all targeted compounds is critical. To accomplish this, a CCD experiment was performed to evaluate and optimize DART parameters. CCD is a type of a formal design of experiment (DoE), which allows efficient multivariate modeling of all selected independent variables enabling not only the response optimum to be found but also the interactions between those variables.[29] The basis of CCD is that the measured response is dependent on several factors, or independent variables, which can be controlled in a range of operable conditions.[28,33] In our experimental design, we selected three variables (plasma temperature, electric grid voltage and interface pressure) with three levels. These levels include two end points near the end of the operable DART conditions and a center point, which can be visualized as −1, 0, and +1 (or in the case of electric grid voltage, −100, −200, and −300 V). To ensure the integrity of the design along the entire studied region, it is important to ensure rotability, meaning the prediction error needs to be the same for two points that are the same distance from the center point. This is accomplished through proper introduction of axial or "star" points. For a three-factor circumscribed CCD, this is calculated as $\alpha = \sqrt[4]{8} = 1.68$. This value, also tested in both the positive and negative space, is then tested for each variable. In the case of electric grid voltage, the values tested are −33 and −367 V. The experimental design is presented in Table S4. All variables tested in the CCD are shown in Table S5 totaling 8 experiments evaluated at each chosen level, 6 experiments for axial points, and 6 central point values (0,0,0). These 20 experiments were performed in triplicate; 2 independent CCDs were performed using helium and nitrogen plasma. As helium was found to permit higher sensitivity, initial discussion on the CCD results highlights the interactions associated with helium. Results for GenX and PFOS ionization in helium

https://doi.org/10.1021/jasms.3c00088
J. Am. Soc. Mass Spectrom. 2023, 34, 1890−1897

plasma are demonstrated in Figure 1, with the Vapur interface pressure set at 897 mbar. Pressure was measured at the interface capillary; results from pressure optimization *vs* plasma temperature for GenX are found in Figure S5. The response was found to be greater with increasingly stronger vacuum, almost doubling with pressure changes as small as 17 mbar.

The fitted response surfaces of GenX in Figure 1 and PFOA in Figure S6 demonstrate that the response of carboxylic acid PFAS is highly dependent on the voltage of the DART electric grid. The lower the absolute voltage value, the greater the response that is obtained. This can also be observed in the corresponding Pareto charts (Figures 1 and S6, respectively), each parameter above $p = 0.05$ being a significant factor in the response of the model analyte. Optimal electric grid voltage values are significantly lower than conventional voltages used for DART (absolute voltage values within 300 and 400 V), a parameter seldomly optimized in literature. This trend has also been observed in the DART-MS analysis of positive ion species,[34] it being posited that the voltage applied to the electric grid could negatively affect the transmission of ions to the MS inlet. Comparing the mass spectra obtained for GenX between the two end points at −100 and −300 V (Figure S7), the $[M - H]^-$ ion is unable to be discriminated from noise at −300 V (m/z = 329) but is readily apparent at −100 V. This voltage played a very minor role in the response of sulfonic acids (Figures 1 and S8); higher response values were obtained with lower absolute voltage but were not statistically significant in the CCD. An optimal electric grid voltage of −50 V was chosen for all model analytes.

For plasma heater temperature, it should be mentioned that the nominal temperature recorded is the temperature of the DART ceramic heater, not the plasma stream. Measured at sample position, the temperature of the helium plasma is 122 °C with the nominal temperature set at 200 °C. To achieve a similar temperature with nitrogen, a plasma heater temperature value of 400 °C is necessary to achieve a 127 °C plasma stream, due to nitrogen's lower heat capacity. The plasma heater temperature was found to be quite significant in response for PFOS, with no significant response on the quantitative ion of the other model analytes. In contrast to the other PFAS targeted, it was observed that both the sulfonic acid functionality and the length of the carbon chain of PFOS are reliant on a high plasma temperature to ionize efficiently. Moreover, the profile of the ion chronogram of PFOS was negatively impacted by lower temperatures due to slower desorption into the ionizing gas from the QuickStrip (Figure S9). At the higher tested plasma temperatures, the responses of GenX and PFOA are slightly reduced, most likely due to their proclivity for decarboxylation and subsequent fragmentation. This is in line with past literature describing that plasma heater temperatures up to 380 °C were not detrimental to the $[M - H]^-$ response of PFOA but resulted in an increased response of the fragment $[M - HCF_2O]^-$.[23] Most likely, the $[M - H]^-$ response is able to be preserved even with enhanced fragmentation due to the increased ionization efficiency of the heated plasma stream. In light of these results, it was decided that optimal values for the plasma heater temperature for the carboxylic acids and sulfonic acids were 250 and 400 °C, respectively.

The gap between the DART and MS inlet in many cases requires a negative pressure interface to better focus the plasma stream and limit the amount of gas into the MS. This is operated by a membrane pump attached to the interface. Interface pressure was optimized between 897 and 931 mbar to evaluate the importance of analyte transmissivity in the plasma stream and to investigate potential interactions with other parameters studied. Interface pressure was found to play a significant role in response for all analytes, most interestingly for GenX and PFOS. As can be seen in the Pareto chart of Figure 1, interface pressure is the most significant influence on the response of GenX. However, there is also a statistically significant positive interaction between interface pressure and electric grid voltage (denoted by 1Lby3L in the Pareto chart). This implies that the influence of the electric grid voltage on GenX is at least partially related to the transmissivity of analyte. Likewise for PFOS, which exhibited a strong preference for high plasma temperature, there is an interaction between interface pressure and plasma temperature (denoted by 2Lby3L on the Pareto chart). This again suggests that plasma temperature plays a major role in the transmissivity of the analyte from the sample to the MS inlet. Optimal conditions for all model analytes were found to be at 897 mbar.

Nitrogen ionizing gas is commonly used as a cheaper and greener alternative to helium to generate plasma; however, its excited state's ionization energy is significantly lower than helium's at 19.8 eV.[35] This can often result in lower ionization efficiency, thus the response. Despite this, the lower ionization energy can also be beneficial, as it can reduce the amount of background interferences that can be ionized. The CCD performed with nitrogen plasma (Figure S10) demonstrated a lower response for all model analytes; however, the amount of background interferences was also reduced (Figure S11). Moreover, the relative intensities of the $[M - H]^-$ of PFOA (413 m/z) and $[M - H - CO_2]^-$ of GenX (285 m/z) were increased compared to their fragments, indicating a softer ionization. Comparing this CCD to that of helium, electric grid voltage plays a statistically significant effect at low absolute values for all model analytes. Surprisingly, GenX demonstrated a strong negative correlation with higher plasma temperature compared to the results observed with helium. This could be due to the increased prevalence of the $[M - H]^-$ and $[M - H - CO_2]^-$ species when using nitrogen, these ions then being quickly fragmented at high plasma temperatures. Plasma heater temperature was not statistically significant for PFOS response; results are shown in Figure S10. This could be attributed to the heat capacity of nitrogen, as the highest tested plasma heater temperature is unable to sufficiently heat nitrogen for proper PFOS desorption. Due to the reduced background, nitrogen is an ideal alternative as an ionizing gas for carboxylic acids; however, ionization efficiency could be poor for the more temperature-dependent sulfonic acids. Due to the Jump Shot capabilities of the DART-JS model used for quantification, the consumption of helium can be reduced by up to 95% in some cases.

Sample Preparation. Previous work in our laboratory has demonstrated that HLB-WAX/PAN SPME devices are ideal for the preconcentration of PFAS prior to instrumental analysis.[15,26] This work utilized SPME thin films coated on stainless-steel blades, as they provide better extraction efficiency than SPME fibers for PFAS.[26] Initial experiments showed no direct desorption of PFAS from SPME devices (fibers and blades) via DART, as the plasma stream was unable to disrupt the ion-exchange interaction between the analytes and the device's extraction phase. Desorption from SPME devices into DART plasma has been demonstrated in other works, utilizing neutral extraction phases.[36−39] Therefore, a

https://doi.org/10.1021/jasms.3c00088
J. Am. Soc. Mass Spectrom. 2023, 34, 1890−1897

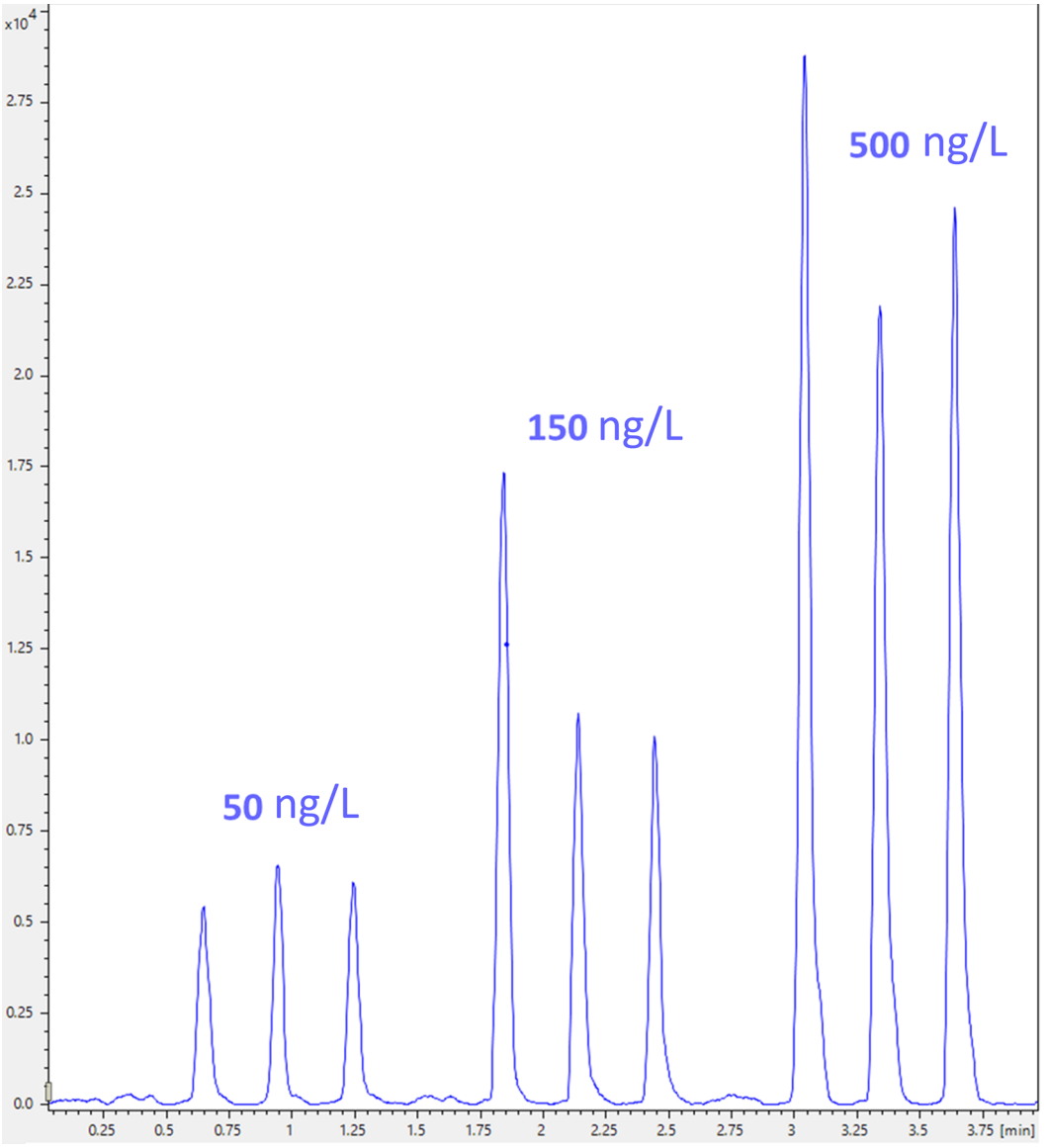

Figure 2. Ion chronogram of PFOA for the concentration range of 50−500 ng/L, analyzed in triplicate with a blank QuickStrip spot between each concentration level. Variability in response is corrected by the internal standard C^{13}−PFOA.

liquid desorption step was carried out before DART analysis in 80:20 methanol:water. While ammonium hydroxide was optimized as the best additive for SPME desorption for the model analytes when analyzed through LC-MS/MS,[15] ammonium formate has also demonstrated to be effective as a desorption additive when analyzing a larger range of PFAS.[26] Results in Figure S12 indicate that the presence of these additives increases the response substantially for sulfonic acids, particularly with the addition of ammonium formate. As negative DART ionization is believed to be initiated by thermal electrons in ambient conditions; the addition of dopants such as different solvents or salts can play a major role in method sensitivity.[40]

Method Performance. SPME extractions from ultrapure water were performed to generate calibration curves, and extracts were analyzed via DART JS hyphenated to a triple quadrupole, Bruker EVOQ Elite, for enhanced sensitivity, using tandem mass spectrometry. Calibration levels at concentrations of 5, 10, 25, 50, 150, 500, 1000, 2500, and 5000 ng/L were analyzed in triplicate with accuracy points at concentrations of 30, 300, and 3000 ng/L. Results in Figure 2 demonstrate calibration curves for each model analyte using helium plasma. Three isotopically labeled PFAS were spiked as internal standards at 750 ng/L for each concentration level. Results indicate excellent linearity for all model analytes, with linear dynamic ranges of the carboxylic acids being broader than the sulfonic acids (PFOA: 10−5000, GenX: 50−5000, PFOS: 50−2500, PFBS: 25−2500 ng/L). Repeatability was below 10% relative standard deviation for the majority of calibration levels with the exception of PFBS. An example of an ion chronogram acquired at varying concentrations between 50 and 500 ng/L is shown in Figure 2 for PFOA. While each sample spotting on the QuickStrip exhibited excellent profile shape and discrimination from noise, it should be noted that the response variability can be easily corrected by proper internal standard selection. As PFBS was the only analyte without an isotopically labeled mechanism available for analysis, other internal standards were tested. Results overall demonstrate poor signal correction, although the internal standard $^{13}C_3$−GenX corrected PFBS better than $^{13}C_8$−PFOS

https://doi.org/10.1021/jasms.3c00088
J. Am. Soc. Mass Spectrom. 2023, 34, 1890−1897

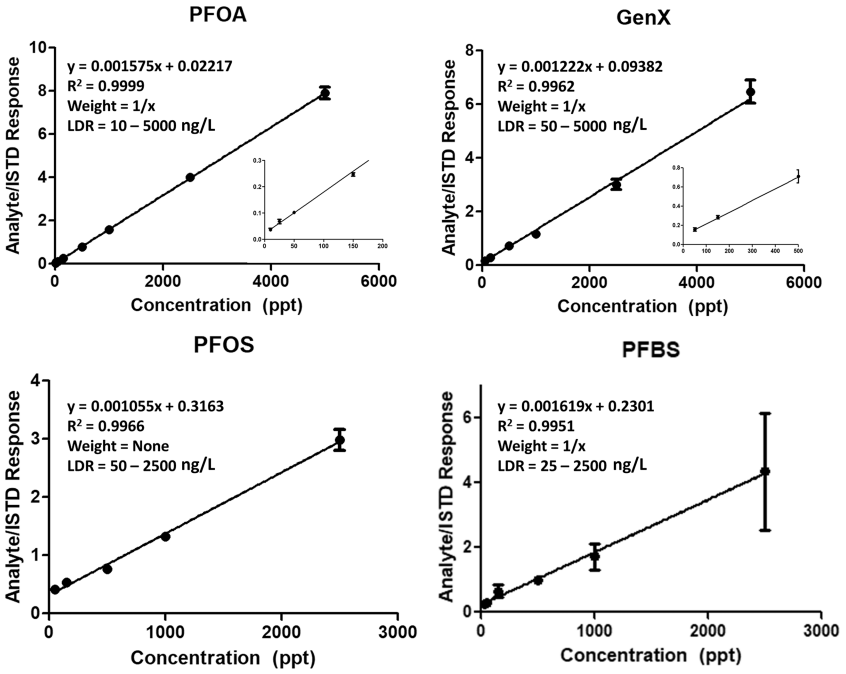

Figure 3. Calibration curves of all analytes using the developed SPME-DART-MS approach.

due to its shorter chain length. Ionization variability can greatly differ with molecules of different physicochemical properties; in this case, each model analyte requires a different internal standard for robust quantification. Calibration curves for each analyte are presented in Figure 3; limits of quantification (LOQ) were all calculated as the lowest point of the calibration curve, which exhibited signal-to-noise (S/N) values above 10 (Table 1). Moreover, the accuracy and reproducibility were evaluated for each accuracy point within the calibration range. With the exception of PFBS, all analytes demonstrated accuracy between 80−120% and reproducibility less than 20% relative standard deviation (Table S6). While $^{13}C_3$ GenX was able to correct for most of the variability of PFBS within the calibration curve experiment, it was unable to correct for the accuracy points, analyzed after the calibration curve acquisition. This further illustrates not only the importance of internal standard selection but also the unique ionization mechanism of each PFAS.

Table 1. Method Performance of the SPME-DART-MS/MS Utilizing Helium Plasma

Model Analyte	LDR (ng/L)	R^2	LOQ (ng/L)	S/N[a]	Weight
PFOA	10−5000	0.999	10	12.0	$1/x$
GenX	50−5000	0.996	50	10.1	$1/x$
PFOS	50−2500	0.997	50	13.9	-
PFBS[b]	25−2500	0.995	25	18.2	-

[a]Signal-to-noise (S/N) is calculated at LOQ of each calibration using the ASTM method. [b]Accuracy points inadequate to verify robustness of calibration curve.

CONCLUSIONS

This study evaluated the robustness of SPME-DART-MS/MS for the quantification of multiclass PFAS by using a multivariate approach, enabling a better understanding of the parameters which affect PFAS ionization and introduction to the MS inlet. All model analytes studied exhibited different behavior and variable interactions in the developed CCD due to their differing physicochemical properties. These results indicate the need for parameter optimization of multiclass analytes when developing these methods, as small differences in chemical structure can significantly influence variable interactions. The developed method allows robust quantification of PFAS enabled through SPME coupled to DART-MS; however, it was observed that the selection of isotopically labeled internal standards is especially critical as even a small change in physiochemical properties can create unique variability in the ionization process. Moving forward, the hyphenation of DART to high-resolution mass spectrometry would allow better sensitivity and screening potential, the use of Kendrick mass defect analysis being essential in this effort.

ASSOCIATED CONTENT

Supporting Information

The Supporting Information is available free of charge at https://pubs.acs.org/doi/10.1021/jasms.3c00088.

Model analytes; structures of PFAS; mass spectrometer parameters; HLB/WAX structure; QuickStrip spiking; DART parameters; CCD parameters; in-source fragmentation; CCD values; interface pressure; PFOA CCD; mass spectra at different voltages; PFBS CCD; temperature effects; nitrogen plasma CCD; helium and nitrogen comparison; additive effects; accuracy points (PDF)

AUTHOR INFORMATION

Corresponding Author

Emanuela Gionfriddo − *Department of Chemistry, Dr. Nina McClelland Laboratory for Water Chemistry and Environmental Analysis, and School of Green Chemistry and Engineering, The University of Toledo, Toledo, Ohio 43606, United States;* orcid.org/0000-0002-1836-1950; Email: Emanuela.Gionfriddo@utoledo.edu

https://doi.org/10.1021/jasms.3c00088
J. Am. Soc. Mass Spectrom. 2023, 34, 1890−1897

Authors

Ronald V. Emmons − *Department of Chemistry and Dr. Nina McClelland Laboratory for Water Chemistry and Environmental Analysis, The University of Toledo, Toledo, Ohio 43606, United States*

William Fatigante − *Bruker Scientific LLC, Billerica, Massachusetts 01821, United States*

Aghogho A. Olomukoro − *Department of Chemistry and Dr. Nina McClelland Laboratory for Water Chemistry and Environmental Analysis, The University of Toledo, Toledo, Ohio 43606, United States*

Brian Musselman − *Bruker Scientific LLC, Billerica, Massachusetts 01821, United States*

Complete contact information is available at: https://pubs.acs.org/10.1021/jasms.3c00088

Author Contributions

The manuscript was written through contributions of all authors. All authors have given approval to the final version of the manuscript.

Notes

The authors declare no competing financial interest.

■ ACKNOWLEDGMENTS

This project was funded in part by the National Oceanic and Atmospheric Administration (NOAA), award # NA18OAR4170100 (Ohio Sea Grant College Program R/PS-056 subaward # 60074859), the NSF CAREER grant #2144591, and further supported by the American Chemical Society Division of Analytical Chemistry Graduate Fellowship Program sponsored by PittCon.

■ REFERENCES

(1) Sunderland, E. M.; Hu, X. C.; Dassuncao, C.; Tokranov, A. K.; Wagner, C. C.; Allen, J. G. A Review of the Pathways of Human Exposure to Poly- and Perfluoroalkyl Substances (PFASs) and Present Understanding of Health Effects. *J. Expo. Sci. Environ. Epidemiol.* **2019**, *29* (2), 131−147.

(2) Xiao, F. Emerging Poly- and Perfluoroalkyl Substances in the Aquatic Environment: A Review of Current Literature. *Water Res.* **2017**, *124*, 482−495.

(3) Tian, Q.; Sun, M. Analysis of GenX and Other Per- and Polyfluoroalkyl Substances in Environmental Water Samples. *Evaluating Water Quality to Prevent Future Disasters* **2019**, *11*, 355.

(4) Janda, J.; Nödler, K.; Brauch, H. J.; Zwiener, C.; Lange, F. T. Robust Trace Analysis of Polar (C2-C8) Perfluorinated Carboxylic Acids by Liquid Chromatography-Tandem Mass Spectrometry: Method Development and Application to Surface Water, Groundwater and Drinking Water. *Environ. Sci. Pollut. Res.* **2019**, *26* (8), 7326−7336.

(5) Lind, L.; Zethelius, B.; Salihovic, S.; Van Bavel, B.; Lind, P. M. Circulating Levels of Perfluoroalkyl Substances and Prevalent Diabetes in the Elderly. *Diabetologia* **2014**, *57* (3), 473−479.

(6) Cousins, I. T.; DeWitt, J. C.; Glüge, J.; Goldenman, G.; Herzke, D.; Lohmann, R.; Miller, M.; Ng, C. A.; Scheringer, M.; Vierke, L.; Wang, Z. Strategies for grouping per- and polyfluoroalkyl substances (PFAS) to protect human and environmental health. *Environmental Science Processes & Impacts* **2020**, *22*, 1444−1460.

(7) Kwiatkowski, C. F.; Andrews, D. Q.; Birnbaum, L. S.; Bruton, T. A.; Dewitt, J. C.; Knappe, D. R. U.; Maffini, M. V; Miller, M. F.; Pelch, K. E.; Reade, A.; Soehl, A.; Trier, X.; Venier, M.; Wagner, C. C.; Wang, Z.; Blum, A. Scientific Basis for Managing PFAS as a Chemical Class. *Environ. Sci. Technol. Lett.* **2020**, *7*, 532.

(8) Mulabagal, V.; Liu, L.; Qi, J.; Wilson, C.; Hayworth, J. S. A Rapid UHPLC-MS/MS Method for Simultaneous Quantitation of 23 Perfluoroalkyl Substances (PFAS) in Estuarine Water. *Talanta* **2018**, *190* (May), 95−102.

(9) World Health Organization. Draft Guidelines for PFOA and PFOS. https://www.who.int/teams/environment-climate-change-and-health/water-sanitation-and-health/chemical-hazards-in-drinking-water/per-and-polyfluoroalkyl-substances.

(10) US Environmental Protection Agency. *Per- and Polyfluoroalkyl Substances (PFAS): Perfluorooctanoic Acid (PFOA) and Perfluorooctanesulfonic Acid (PFOS) National Primary Drinking Water Regulation Rulemaking*; 2023.

(11) Cousins, I. T.; Dewitt, J. C.; Glüge, J.; Goldenman, G.; Herzke, D.; Lohmann, R.; Ng, C. A.; Scheringer, M.; Wang, Z. The High Persistence of PFAS Is Sufficient for Their Management as a Chemical Class. *Environ. Sci. Process. Impacts* **2020**, *22* (12), 2307−2312.

(12) Yang, L.-H.; Yang, W.-J.; Lv, S.-H.; Zhu, T.-T.; Adeel Sharif, H. M.; Yang, C.; Du, J.; Lin, H. Is HFPO-DA (GenX) a Suitable Substitute for PFOA? A Comprehensive Degradation Comparison of PFOA and GenX via Electrooxidation. *Environ. Res.* **2022**, *204*, 111995.

(13) Nakayama, S. F.; Yoshikane, M.; Onoda, Y.; Nishihama, Y.; Iwai-Shimada, M.; Takagi, M.; Kobayashi, Y.; Isobe, T. Worldwide Trends in Tracing Poly- and Perfluoroalkyl Substances (PFAS) in the Environment. *TrAC - Trends Anal. Chem.* **2019**, *121*, 115410.

(14) Jahnke, A.; Berger, U. Trace Analysis of Per- and Polyfluorinated Alkyl Substances in Various Matrices-How Do Current Methods Perform? *J. Chromatogr. A* **2009**, *1216* (3), 410−421.

(15) Olomukoro, A. A.; Emmons, R. V.; Godage, N. H.; Cudjoe, E.; Gionfriddo, E. Ion Exchange Solid Phase Microextraction Coupled to Liquid Chromatography/Laminar Flow Tandem Mass Spectrometry for the Determination of Perfluoroalkyl Substances in Water Samples. *J. Chromatogr. A* **2021**, *1651*, No. 462335.

(16) Cooks, R. G.; Ouyang, Z.; Takats, Z.; Wiseman, J. M. Ambient Mass Spectrometry. *Science (80-.)* **2006**, *311* (5767), 1566−1570.

(17) Sisco, E.; Verkouteren, J.; Staymates, J.; Lawrence, J. Rapid Detection of Fentanyl, Fentanyl Analogues, and Opioids for on-Site or Laboratory Based Drug Seizure Screening Using Thermal Desorption DART-MS and Ion Mobility Spectrometry. *Forensic Chem.* **2017**, *4*, 108−115.

(18) Lesiak, A. D.; Musah, R. A. Application of Ambient Ionization High Resolution Mass Spectrometry to Determination of the Botanical Provenance of the Constituents of Psychoactive Drug Mixtures. *Forensic Sci. Int.* **2016**, *266* (2016), 271−280.

(19) Jastrzembski, J. A.; Sacks, G. L. Solid Phase Mesh Enhanced Sorption from Headspace (SPMESH) Coupled to DART-MS for Rapid Quantification of Trace-Level Volatiles. *Anal. Chem.* **2016**, *88* (17), 8617−8623.

(20) Rýdlová, L.; Prchalová, J.; Škorpilová, T.; Rohlík, B. A.; Čížková, H.; Rajchl, A. Evaluation of Cocoa Products Quality and Authenticity by DART/TOF-MS. *Int. J. Mass Spectrom.* **2020**, *454*, 116358.

(21) Zabalegui, N.; Manzi, M.; Depoorter, A.; Hayeck, N.; Roveretto, M.; Li, C.; Van Pinxteren, M.; Herrmann, H.; George, C.; Monge, M. E. Seawater Analysis by Ambient Mass-Spectrometry-Based Seaomics. *Atmos. Chem. Phys.* **2020**, *20* (10), 6243−6257.

(22) Bai, Y.; Zhang, J.; Bai, Y.; Liu, H. Direct Analysis in Real Time Mass Spectrometry Combined with Single-Drop Liquid-Liquid-Liquid Microextraction for the Rapid Analysis of Multiple Phytohormones in Fruit Juice. *Anal. Bioanal. Chem.* **2012**, *403* (8), 2307−2314.

(23) Cody, R.; Maleknia, S. D. Coated Glass Capillaries as SPME Devices for DART Mass Spectrometry. *Rapid Commun. Mass Spectrom.* **2020**, *34* (23), e8946.

(24) Li, X.; Ma, W.; Li, H.; Ai, W.; Bai, Y.; Liu, H. Sampling and Analyte Enrichment Strategies for Ambient Mass Spectrometry. *Anal. Bioanal. Chem.* **2018**, *410* (3), 715−724.

(25) Albert, A.; Shelley, J. T.; Engelhard, C. Plasma-Based Ambient Desorption/Ionization Mass Spectrometry: State-of-the-Art in Qual-

itative and Quantitative Analysis. *Anal. Bioanal. Chem.* **2014**, *406* (25), 6111−6127.
(26) Olomukoro, A. A.; DeRosa, C.; Gionfriddo, E. Investigation of the Adsorption/Desorption Mechanism of Perfluoroalkyl Substances on HLB-WAX Extraction Phases for Microextraction. *Anal. Chim. Acta* **2023**, *1260*, 341206.
(27) Lawson, J. *Design and Analysis of Experiments with R*; Chapman and Hall/CRC, 2015.
(28) Zhang, Z.; Xiaofeng, B. Comparison about the Three Central Composite Designs with Simulation. *Proc. - Int. Conf. Adv. Comput. Control. ICACC 2009* **2009**, No. 3, 163−167.
(29) Marrubini, G.; Dugheri, S.; Cappelli, G.; Arcangeli, G.; Mucci, N.; Appelblad, P.; Melzi, C.; Speltini, A. Experimental Designs for Solid-Phase Microextraction Method Development in Bioanalysis: A Review. *Anal. Chim. Acta* **2020**, *1119*, 77−100.
(30) Lyon, P. A.; Tomer, K. B.; Gross, M. L. Fast Atom Bombardment and Tandem Mass Spectrometry for Characterizing Fluoroalkanesulfonates. *Anal. Chem.* **1985**, *57* (14), 2984−2989.
(31) Arsenault, G.; McAlees, A.; McCrindle, R.; Riddell, N. Analysis of Perfluoroalkyl Anion Fragmentation Pathways for Perfluoroalkyl Carboxylates and Sulfonates during Liquid Chromatography/Tandem Mass Spectrometry: Evidence for Fluorine Migration Prior to Secondary and Tertiary Fragmentation. *Rapid Commun. Mass Spectrom.* **2007**, *21* (23), 3803−3814.
(32) Brase, R. A.; Spink, D. C. Enhanced Sensitivity for the Analysis of Perfluoroethercarboxylic Acids Using LC-ESI-MS/MS: Effects of Probe Position, Mobile Phase Additive, and Capillary Voltage. *J. Am. Soc. Mass Spectrom.* **2020**, *31* (10), 2124−2132.
(33) Box, G. E. P.; Wilson, K. B. On the Experimental Attainment of Optimum Conditions. *J. R. Stat. Soc. Ser. B* **1951**, *13* (1), 1−38.
(34) Emmons, R. V.; Gionfriddo, E. Minimizing Transient Microenvironment-Associated Variability for Analysis of Environmental Anthropogenic Contaminants via Ambient Ionization - Supplemental Information. *Sci. Total Environ.* **2021**, *775*, 1−5.
(35) Cody, R. B.; Laramée, J. A.; Durst, H. D. Versatile New Ion Source for the Analysis of Materials in Open Air under Ambient Conditions. *Anal. Chem.* **2005**, *77* (8), 2297−2302.
(36) Emmons, R. V.; Gionfriddo, E. Minimizing Transient Microenvironment-Associated Variability for Analysis of Environmental Anthropogenic Contaminants via Ambient Ionization. *Sci. Total Environ.* **2021**, *775*, No. 145789.
(37) Newsome, G. A.; Kavich, G.; Alvarez-Martin, A. Interface for Reproducible, Multishot Direct Analysis of Solid-Phase Microextraction Samples. *Anal. Chem.* **2020**, *92* (6), 4182−4186.
(38) Vasiljevic, T.; Gómez-Ríos, G. A.; Pawliszyn, J. Single-Use Poly(Etheretherketone) Solid-Phase Microextraction-Transmission Mode Devices for Rapid Screening and Quantitation of Drugs of Abuse in Oral Fluid and Urine via Direct Analysis in Real-Time Tandem Mass Spectrometry. *Anal. Chem.* **2018**, *90* (1), 952−960.
(39) Watt, L.; Sisco, E. Detection of Trace Drugs of Abuse in Baby Formula Using Solid-Phase Microextraction Direct Analysis in Real-Time Mass Spectrometry (SPME-DART-MS). *J. Forensic Sci.* **2021**, *66* (1), 172−178.
(40) Dousty, F.; O'Brien, R. The Use of Isoprene as a Novel Dopant in Negative Ion Atmospheric Pressure Photoionization Mass Spectrometry Coupled to High-Performance Liquid Chromatography. *Rapid Commun. Mass Spectrom.* **2015**, *29* (11), 1031−1038.

https://doi.org/10.1021/jasms.3c00088
J. Am. Soc. Mass Spectrom. 2023, 34, 1890−1897